EUROPEAN ORGANIZATION FOR NUCLEAR RESEARCH

Contribution to session B7E

MEASUREMENT OF THE LIFETIME AND BRANCHING RATIOS OF THE Ω^-

Bristol[1], Geneva[2], Heidelberg[3], Orsay[4], Rutherford[5], Strasbourg[6] Collaboration

M. Bourquin[2], R.M. Brown[5], Y. Chatelus[6], J.C. Chollet[4], A. Degré[6], D. Froidevaux[4], A.R. Fyfe[1], C.N.P. Gee[5], J.M. Gaillard[4], M. Gibson[1], P. Igo-Kemenes[3], P.W. Jeffreys[1], B. Merkel[4], R. Morand[6], H. Plothow*, J.P. Repellin[4], B.J. Saunders[5], G. Sauvage[4], B. Schiby[6], H.W. Siebert[3], V.J. Smith[1], K.P. Streit[3], R. Strub[6], J.J. Thresher[5]

ABSTRACT

A sample of about 2000 reconstructed Ω^- decays has been collected in the CERN-SPS charged hyperon beam. Events are selected by a DISC Čerenkov counter. Charged decay products are measured by a magnetic spectrometer and gamma rays are measured in lead glass and lead scintillator detectors.

The lifetime is determined using the $\Omega^- \to \Lambda K^-$ mode. The $\Omega^- \to \Xi^0\pi^-/\Omega^- \to \Lambda K^-$ and $\Omega^- \to \Xi^-\pi^0/\Omega^- \to \Lambda K^-$ branching ratios are determined. We have searched for semi-leptonic decay modes using the electron signature provided by transition radiation and lead glass detectors, and also for other rare decays.

Geneva

July 1978

---

1 H.H. Wills Physics Laboratory, University of Bristol, Bristol (England)

2 University of Geneva (Switzerland)

3 Physikalisches Institut, Heidelberg Universität, Philosophenweg 12, D-6900 Heidelberg (Germany)

4 Laboratoire de l'Accélerateur Linéaire, Centre d'Orsay, 91405 Orsay (France)

5 Rutherford Laboratory, Chilton, Didcot, Oxon Ox11 0QX (England)

6 C.R.N. - Division des Hautes Energies, 67037 Strasbourg-Cedex (France)

* CERN Fellow, 1211 Geneva 23 (Switzerland)

INTRODUCTION

The Ω^- particle was predicted by Gell-Mann and Néeman in 1961 and seen first of all at BNL in 1964. Until 1978, bubble chamber experiments had collected a total of only about 160 events. These experiments have given conflicting lifetime measurements and very little information about branching ratios[1]. In 1977 the first operation of the CERN-SPS charged hyperon beam established the existence of a significant flux of Ω^- in the hyperon secondary beam channel.[2] This paper presents preliminary results of the analysis of 2/3 of the data taken in 1978 during a 25-day running period.

1. THE MEASUREMENT OF THE Ω^- DECAY

The 210 GeV/c primary proton beam interacts in a BeO target. The hyperon magnetic channel selects the particles produced at 0^o into a $\pm$ 8% momentum bite centered at 98.5 GeV/c. Typically, with $3 \cdot 10^{10}$ protons per burst on the target, we produce 10^6 particles at the exit of the channel. The apparatus (fig. 1) being described in another contribution to this Conference[2], we restrict the description to the special features of the Ω^- experiment. To trigger on Ω^- decays, we require a coincidence between the signals delivered by:

(i) A DISC counter, whose pressure is set to select 98.5 GeV/c Ω^-. The effective channel length to be considered is then 11.2 m, i.e. the distance between the target and the DISC counter.

(ii) A multiplicity counter which requires more than one charged particle 10 m downstream of the DISC. This counter fixes the cut off of the decay region.

(iii) A proton counter which is located downstream of the spectrometer and covers the spot of protons from Λ decays.

With these requirements, the trigger rate is about 12 for 10^6 particles entering the DISC. This rate is further reduced by a factor of 4 when we reject high track multiplicity events using the online computer. Under these conditions, we have collected 360 000 triggers which are still mainly multitrack events or true Ξ^- whose early decay triggered the DISC and fulfilled the other trigger requirements.

2. THE EVENT SELECTION

We have studied the following decay modes where we measure the momenta of all charged particles:

$$\Omega^- \to \Lambda K^-$$
$$\quad\quad \lfloor\!\to\ p\pi^-$$

$$\Omega^- \to \Xi^0\pi^-$$
$$\quad\quad \lfloor\!\to\ \Lambda\pi^0$$
$$\quad\quad\quad \lfloor\!\to\ p\pi^-$$

$$\Omega^- \to \Xi^-\pi^0$$
$$\quad\quad \lfloor\!\to\ \Lambda\pi$$
$$\quad\quad\quad \lfloor\!\to\ p\pi^-$$

$$\Omega^- \to \Lambda\pi^-$$

$$\Omega \to \Xi^-\pi^+\pi^-$$

$$\Omega \to \Xi^0 e^- \bar{\nu}$$

The presence of a Λ particle decaying into a proton and a π^- being a common feature of these channels, the reconstruction program starts the event search by computing the (p, π^-) effective mass and a possible vertex for these two tracks. Only those events having a $(p\ \pi^-)$ effective mass within $\pm$ 10 MeV/c^2 of the Λ mass and a vertex located in the fiducial region are considered for further analysis. For each decay mode, additional cuts are then made to reduce the background, and the efficiency for the signal is determined.

(a) ΛK^- selection

Selection of the (ΛK^-) candidates is made requiring:

- The (Λ, K^-) effective mass = 1672 $\pm$ 50 MeV/c^2
- The momentum balance between the Ω^- momentum, measured to $\pm$ 1% with the beam telescope, and the (Λ, K^-) momentum measured by the spectrometer ($\pm$ 1.5%) is smaller than 10 GeV/c.

For the other Ω^- decay modes we apply an additional cut requiring that the Ω^- decay vertex occurs after the end of the DISC counter, to reduce the background for those decays. Figure 2 shows the scatter plot of the

(ΛK^-) mass versus the ($\Lambda^0\pi^-$) mass with the Ω^- decay vertex cut applied. The projection of the events with a ($\Lambda^0\pi^-$) mass > 1350 MeV/c^2 on the (Λ^0K^-) axis is shown in fig. 3. Within a mass range of ± 10 MeV/c^2 centered at the Ω^- mass there are 1244 events with an estimated background of 20 events. This sample is used for the branching ratio measurement.

For the Ω^- lifetime measurement reported below, the Ω^- decay vertex cut has not been applied, and with the kinematic selection criteria given above we obtain a sample of 1410 events with an estimated background of 23 events. One half of the background is due to $\Omega^- \to \Xi^0\pi^-$ decays, the other half is the residual $\Xi^- \to \Lambda^0\pi^-$ contamination.

(b) $\Xi^0\pi^-$ selection

Selection of the $\Xi^0\pi^-$ candidates is made requiring:

- the ($\Omega^-\pi^-$) missing mass = 1315 ± 150 MeV/c^2
- the Ω^- decay takes place downstream of the end of the DISC counter
- the beam momentum is within ± 10 GeV/c of the mean beam momentum
- the momentum of the missing π^0 is greater than 2 GeV/c.

Figure 4 displays the scatter plot of the ($\Omega^-\pi^-$) missing mass and the (ΛK^-) effective mass: a clear signal appears at the Ξ^0 mass and the main background comes from the $\Omega^- \to \Lambda K^-$ decay. Figure 5 is a projection of these events on the ($\Omega^-\pi^-$) axis. Knowing the background distribution from a study of the ΛK^- events, we obtain after subtraction, a total of 240 ± 22 $\Xi^0\pi^-$ events.

π^0 detection

The experiment includes several photon detectors:

- At the end of the decay region there is a hodoscope of lead scintillator sandwiches which locates the impacts of photons emitted at large angles.
- Downstream of the spectrometer, there are two MWPC's interleaved with lead plates and followed by a three-layer lead glass wall. These devices measure the impact position and energy of forward produced photons.

Requiring the detection of at least one photon in one of these detectors, the background shown on fig. 5 is reduced by a factor of 3, keeping a 90% efficiency on the signal (dashed distribution). Figure 6 shows the π^0 missing mass squared computed for the $\Xi^0\pi^-$ candidates satisfying the one photon requirement.

A further check of the photon detection efficiency is made by inverting the beam polarity and detecting the $\Sigma^+ \to p\pi^0$ decays. From that study we deduce the photon detection efficiency as a function of π^0 momentum (fig. 7). For comparison, the figure also shows the photon detection efficiency measured from the $\Xi^0\pi^-$ events themselves.

Knowledge of the photon detection efficiency is not essential for the study of the $\Omega^- \to \Xi^0\pi^-$ decay, but it is of primary importance for $\Omega^- \to \Xi^-\pi^0$.

(c) $\Xi^-\pi^0$ selection

Selection of the $\Xi^-\pi^0$ candidates is made requiring:

- the (Λ, π^-) effective mass = 1322 ± 15 MeV/c^2
- the beam momentum is within ± 10 GeV/c of the mean beam momentum
- the supposed missing π^0 has a longitudinal momentum p_L greater than 1 GeV/c
- the different decay vertices are ordered as follows:

$$z_{\Omega^-} < z_{\Xi^-} < z_{\Lambda}$$

The background in this sample comes from the $\Xi^- \to \Lambda\pi^-$ events which are mainly concentrated at low p_L (p_L < 10 GeV/c), as shown on fig. 8. The expected correlation between p_L and the $(\Omega^- - \Xi^-)$ missing mass squared is observed for the background contribution. Applying the photon requirement on all candidates, we find that the momentum region below 10 GeV/c is strongly suppressed, while the events at higher momenta are only reduced by a factor 1.4. Figure 9 shows the projection of the events (p_L > 10 GeV/c) on the $(\Omega^- - \Xi^-)$ missing mass squared axis. The hatched events are those which do not satisfy the photon requirements. Using the measured 90% photon detection efficiency and a background rejection of 3.5, we obtain a $\Xi^-\pi^0$ signal of 86 ± 12 events for p_L > 10 GeV/c.

3. Ω^- LIFETIME

The lifetime measurement is done using the $\Omega^- \to \Lambda^0 K^-$ decay mode, which is the most abundant. The event selection has been described in paragraph 2.a. We measure the Ω^- decay vertex distribution. How accurately a lifetime can be deduced from this distribution has been checked by comparing a Monte Carlo (M-C) simulation with the decay vertex distribution of $\Xi^- \to \Lambda^0 \pi^-$ events measured in the same apparatus.

The M-C simulation includes:

- the momentum and spatial distributions of the beam particles
- the trigger requirements
- the tracking of charged particles through the magnet
- the measurement errors
- the effect of confusion between very close tracks in the wire chamber telescope located before the magnet
- the event selection criteria.

The parametrization of the confusion effect in the M-C simulation has been optimized on the $\Xi^- \to \Lambda\pi^-$ decays.

Figure 10 shows the vertex position distribution of the Ξ^- from a sample of 22 000 events. The solid curve shown on the figure is the result of the Monte Carlo. Figure 11 shows the vertex position distribution for the $\Omega^- \to \Lambda K^-$ events. The χ^2 of the fit between the data points and the Monte Carlo tried for different lifetime hypotheses is shown on fig. 12. Taking into account a systematic uncertainty of 0.05×10^{-10} sec we obtain:

$$\tau_{\Omega^-} = (.82 \pm .06) \times 10^{-10} \text{ sec.}$$

This value is stable if the start of the decay region is varied between 175 and 375 cm.

4. BRANCHING RATIOS FOR THE MAIN Ω^- DECAY MODES

Assuming $\Gamma(\Lambda K) + \Gamma(\Xi^0\pi^-) + \Gamma(\Xi^-\pi^0) = \Gamma(\text{all})$, i,e, neglecting rarer decay modes for the present, and knowing the selection efficiency and relative acceptances from the Monte Carlo simulation, we obtain

the following ratios:

$$\frac{\Gamma(\Lambda K)}{\Gamma(\text{all})} = (67.0 \pm 2.2) \times 10^{-2} \qquad \frac{\Gamma(\Xi^0\pi^-)}{\Gamma(\text{all})} = (24.6 \pm 1.9) \times 10^{-2}$$

$$\frac{\Gamma(\Xi^-\pi^0)}{\Gamma(\text{all})} = (8.4 \pm 1.1) \times 10^{-2}$$

The systematic uncertainties being negligible, the quoted uncertainties are statistical only. With these measurements we calculate the ratio

$$\frac{\Gamma(\Xi^0\pi^-)}{\Gamma(\Xi^-\pi^0)} = 2.93 \pm 0.50$$

A pure $\Delta I = \frac{1}{2}$ amplitude would have given a ratio $\Gamma(\Xi^0\pi^-) / \Gamma(\Xi^-\pi^0) = 2$, but a recent theoretical calculation made by J. Finjord[3] predicts $\Gamma(\Xi^0\pi^-) / \Gamma(\Xi^-\pi^0) \simeq 3$ by taking into account a non-negligible contribution of $\Delta I = 3/2$ amplitudes.

5. THE RARE DECAY MODES

The data sample has been analysed for the selection of $\Omega^- \to \Lambda\pi^-$ events. These events correspond to a $\Delta S = -2$ transition which is suppressed by the selection rules. We have found no events and conclude that

$$\frac{\Gamma(\Omega \to \Lambda^0\pi^-)}{\Gamma(\text{all})} < 1.5 \cdot 10^{-3} \text{ at 90\% confidence level.}$$

The decay channel $\Omega^- \to \Xi^-\pi^+\pi^-$ has been analysed. At the present stage of the analysis, 1 clear event has been found with coherent vertices and a (Ξ^-, π^+) effective mass near the $\Xi^*(1530)$ mass. This event corresponds to a branching ratio of $\sim 10^{-3}$.

We have searched for the decay $\Omega^- \to \Xi^0 e^- \bar{\nu}$ followed by $\Xi^0 \to \Lambda^0 + \pi^0$. We have found 3 candidates which have an identified electron, a reconstructed π^0 and correct π^0 and $(\Lambda^0\pi^0)$ masses. We are still investigating possible residual backgrounds from the decays $\Omega^- \to \Xi^0\pi^-$ and $\Omega^- \to \Xi^-\pi^0$. With the relative efficiency for that decay mode, 3 events would correspond to a branching ratio $\Gamma_{\text{lept}} / \Gamma_{\text{all}} \simeq 10^{-2}$.

6. THE DECAY ASYMMETRY PARAMETER α FOR $\Omega^- \to \Lambda K^-$

As we measure completely all the particles involved in the ΛK^- decay we have used these events to compute the weak-decay asymmetry parameter $\alpha_{\Lambda K}$. This parameter describes the interference of the two partial waves $a_{j-\frac{1}{2}}$ and $a_{j+\frac{1}{2}}$ which contribute to the transition matrix. It is a measure of parity violation in that decay. Let θ be the angle between the direction of the proton in the Λ rest frame and the direction of the Λ in the Ω^- rest frame. The angular distribution is given by:

$$I(\cos\theta) \sim 1 + \alpha_\Lambda \alpha_{\Lambda K} \cos\theta$$

Knowing α_Λ ($\alpha_\Lambda = .642 \pm .013$) and fitting the experimental angular distribution with such a representation, we obtain

$$\alpha_{\Omega \to \Lambda K} = .06 \pm .14$$

where we quote the statistical uncertainty only. As a check, we have also measured $\alpha_{\Xi^- \to \Lambda\pi^-}$ and we obtain

$$\alpha_{\Xi^- \to \Lambda\pi^-} = -.312 \pm .078$$

which is in good agreement with the PDG value

$$\alpha_{\Xi^- \to \Lambda\pi^-} = -.392 \pm .021$$

Our measurement is in good agreement with theoretical expectation that the $\Omega^- \to \Lambda K$ decay mode be nearly parity conserving.[4] Earlier analysis of bubble chamber events produced $\alpha_{\Omega \to \Lambda K} = -.66 \pm .36$ (15 events)[5] $\alpha_{\Omega \to \Lambda K} = -.2 \pm .4$ (40 events)[1].

7. CONCLUSION

Study of this large sample (1713 events) of Ω^- decays has provided a precise determination of

(i) The Ω^- lifetime $\tau_{\Omega^-} = (.82 \pm .06)\ 10^{-10}$ sec

(ii) The Ω^- branching ratios into ΛK^-, $\Xi^0\pi^-$, $\Xi^-\pi^0$

$$\frac{\Gamma(\Lambda K)}{\Gamma(\text{all})} = (67.0 \pm 2.2) \cdot 10^{-2} \qquad \frac{\Gamma(\Xi^0\pi^-)}{\Gamma(\text{all})} = (24.6 \pm 1.9)\ 10^{-2}$$

$$\frac{\Gamma(\Xi^-\pi^0)}{\Gamma(\text{all})} = \qquad (8.4 \pm 1.1)\ 10^{-2}$$

(iii) The weak decay asymmetry parameter for $\Omega^- \to \Lambda K^-$

$$\alpha_{\Lambda K} = .06 \pm .14$$

The search for rare decay modes has allowed us to set an upper limit on the $\Delta S = -2$ forbidden transition, $\Omega^- \to \Lambda\pi^-$:

$$\frac{\Gamma(\Omega^- \to \Lambda\pi^-)}{\Gamma(\text{all})} < 1.5 \cdot 10^{-3} \text{ at 90\% confidence level.}$$

REFERENCES

1) Particle data group, Rev. Mod. Phys. 48 (1976) no. 2, part II.
M. Deutschmann et al., Phys. Lett. B73 (1978) 96.
R.J. Hemingway et al., preprint May 1978.

2) Particle and antiparticle production by 200 and 210 GeV protons in the CERN-SPS charged hyperon beam.
Paper submitted at this Conference.

3) J. Finjod, CERN preprint TH 2452.

4) L.R. Ram Mohan, Phys. Rev. D1 (1970) 266.

5) D.J. Kocher and K.L. Wernhard, Phys. Lett. 51B (1974) 193.

FIGURE CAPTIONS

Fig. 1 Apparatus

Fig. 2 Scatter plot of the (Λ, K^-) and $(\Lambda\pi^-)$ effective masses for the candidates to $\Omega^- \to \Lambda K^-$

Fig. 3 (Λ, K^-) effective mass for events with $(\Lambda\pi^-)$ mass > 1.350 GeV/c^2

Fig. 4 Scatter plot of the $(\Omega^- - \pi^-)$ missing mass and the (Λ, K^-) effective mass for the candidates to $\Omega^- \to \Xi^0\pi^-$

Fig. 5 The solid line is the $(\Omega^- - \pi^-)$ missing mass for $\Omega^- \to \Xi^0\pi^-$ candidates. The dashed line is the same distribution for the events which have at least one measured photon.

Fig. 6 π^0 missing mass squared for $\Xi^0\pi^-$ events with at least one measured photon.

Fig. 7 Probability to detect at least one photon as a function of π^0 momentum. The solid line comes from the photon detection efficiency determined on $\Sigma^+ \to p\pi^0$. The points are obtained from $\Omega^- \to \Xi^0\pi^-$

Fig. 8 Correlation between the $(\Omega^- - \Xi^-)$ missing mass squared and the longitudinal momentum of the missing π^0 for $\Omega^- \to \Xi^-\pi^0$ candidates

Fig. 9 $(\Omega^- - \Xi^-)$ missing mass squared for $\Omega^- \to \Xi^-\pi^0$ after elimination of the events with $p_L \leq 10$ GeV/c. The dashed events have no measured photon.

Fig. 10 Vertex position distribution for $\Xi^- \to \Lambda\pi^-$. The solid curve is the result of the Monte Carlo simulation taking $\tau_{\Xi^-} = 1.6 \times 10^{-10}$ sec. The arrows delimit the range of decay points used for the calculation.

Fig. 11 Vertex position distribution for $\Omega^- \to \Lambda K^-$. The solid line is the Monte Carlo result with $\tau_{\Omega^-} = .82 \cdot 10^{-10}$ sec. The arrows delimit the range of decay points used for the calculation.

Fig. 12 χ^2 of the best fit between the data points and the Monte Carlo for different Ω^- lifetime hypotheses

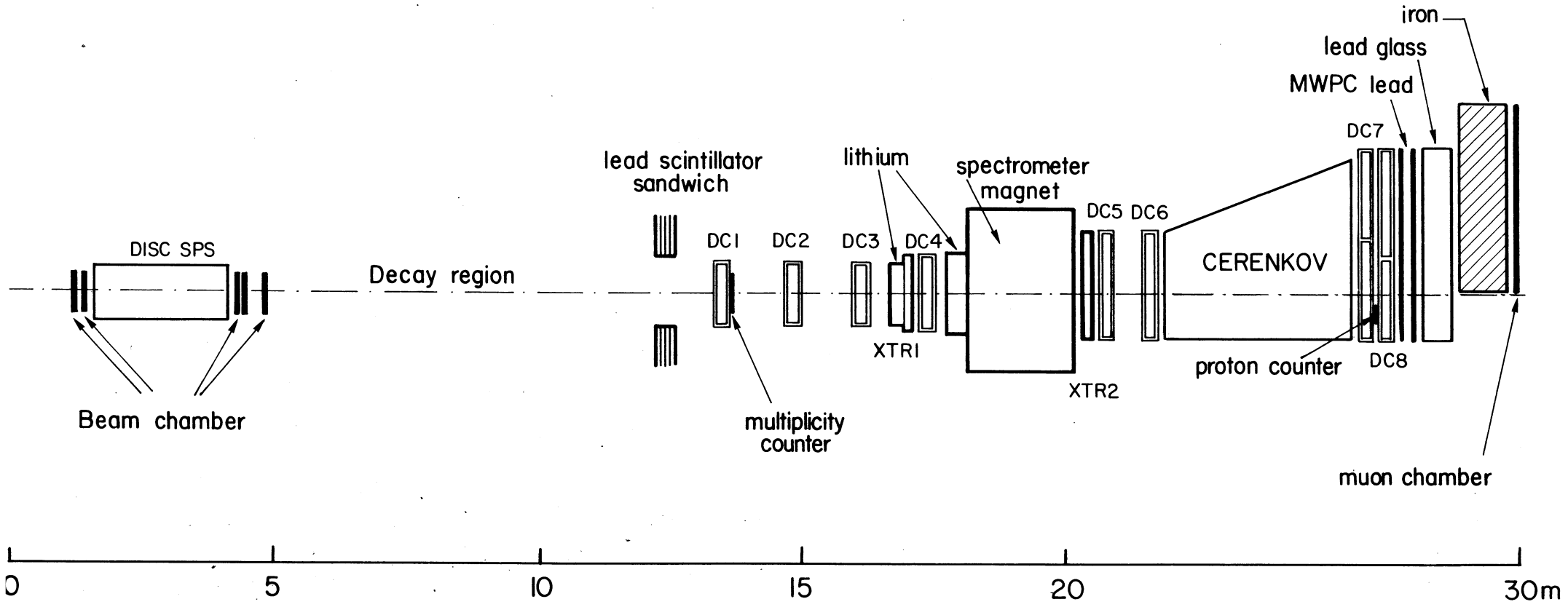
iron
lead glass
MWPC lead
DC7
lead scintillator sandwich
lithium
spectrometer magnet
DC5 DC6
DISC SPS
DC1
DC2
DC3
DC4
CERENKOV
Decay region
XTR1
XTR2
proton counter
DC8
Beam chamber
multiplicity counter
muon chamber
0
5
10
15
20
30m

Fig. 1

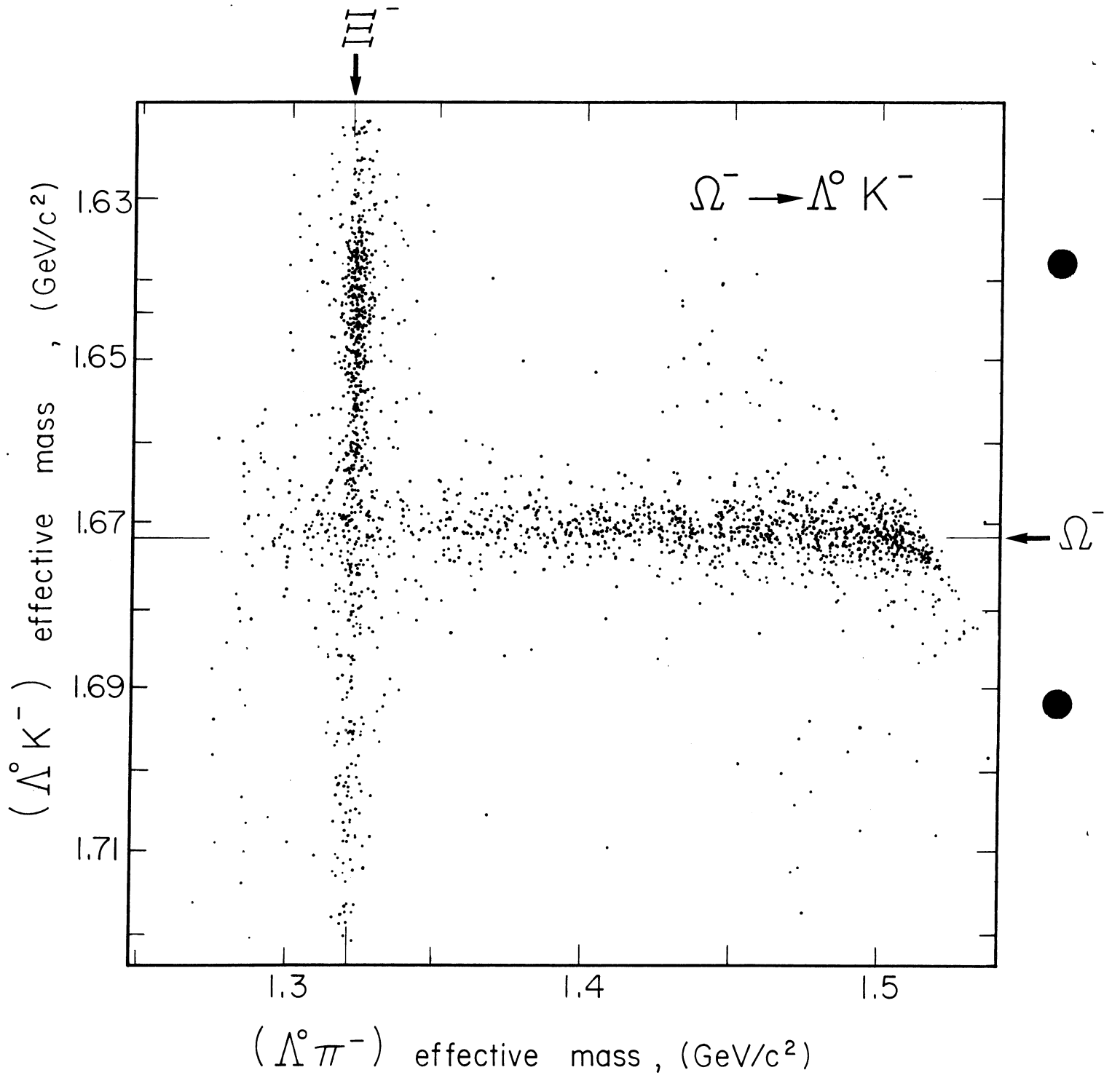
Ξ⁻
Ω⁻ → Λ° K⁻
1.63
1.65
1.67
1.69
1.71
Ω⁻
(Λ° K⁻) effective mass , (GeV/c²)
1.3
1.4
1.5
(Λ° π⁻) effective mass , (GeV/c²)

Fig. 2

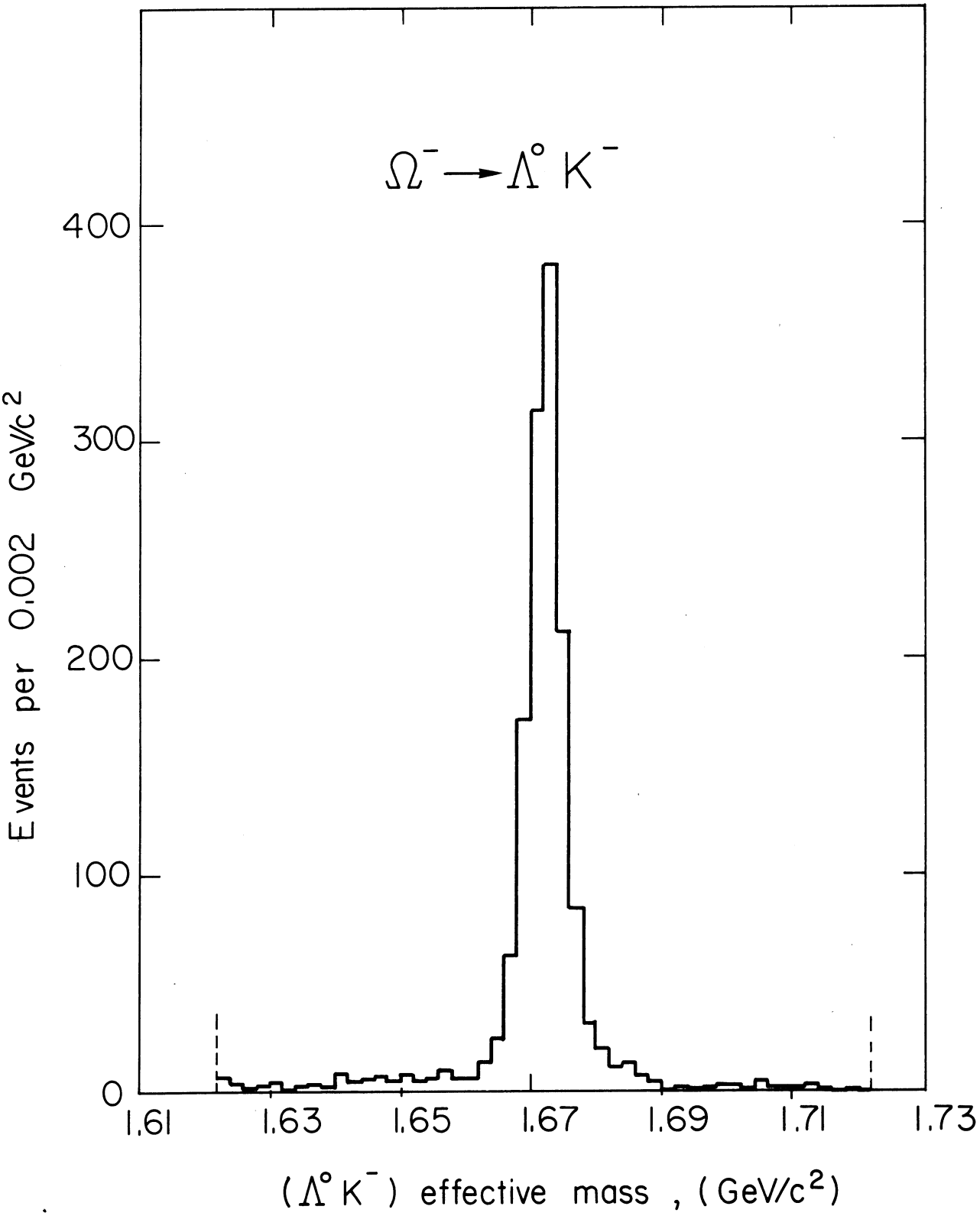
$\Omega^- \rightarrow \Lambda^\circ K^-$
400
300
200
100
0
Events per 0.002 GeV/c^2
1.61
1.63
1.65
1.67
1.69
1.71
1.73
($\Lambda^\circ K^-$) effective mass , (GeV/c^2)

Fig. 3

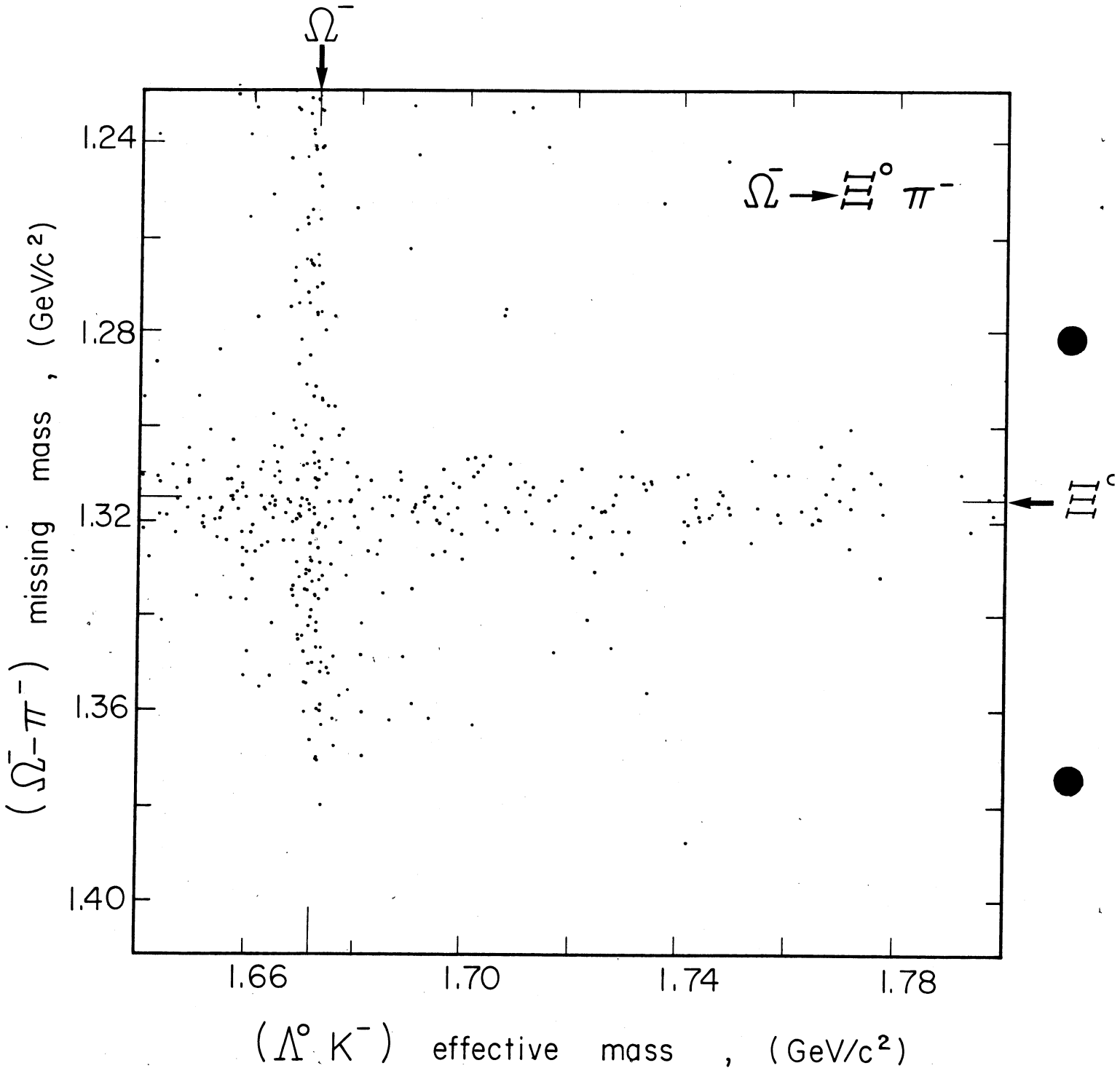
Ω^-
$\Omega^- \to \Xi^\circ \pi^-$
Ξ°
1.24
1.28
1.32
1.36
1.40
$(\Omega^- - \pi^-)$ missing mass , (GeV/c²)
1.66
1.70
1.74
1.78
$(\Lambda^\circ K^-)$ effective mass , (GeV/c²)

Fig. 4

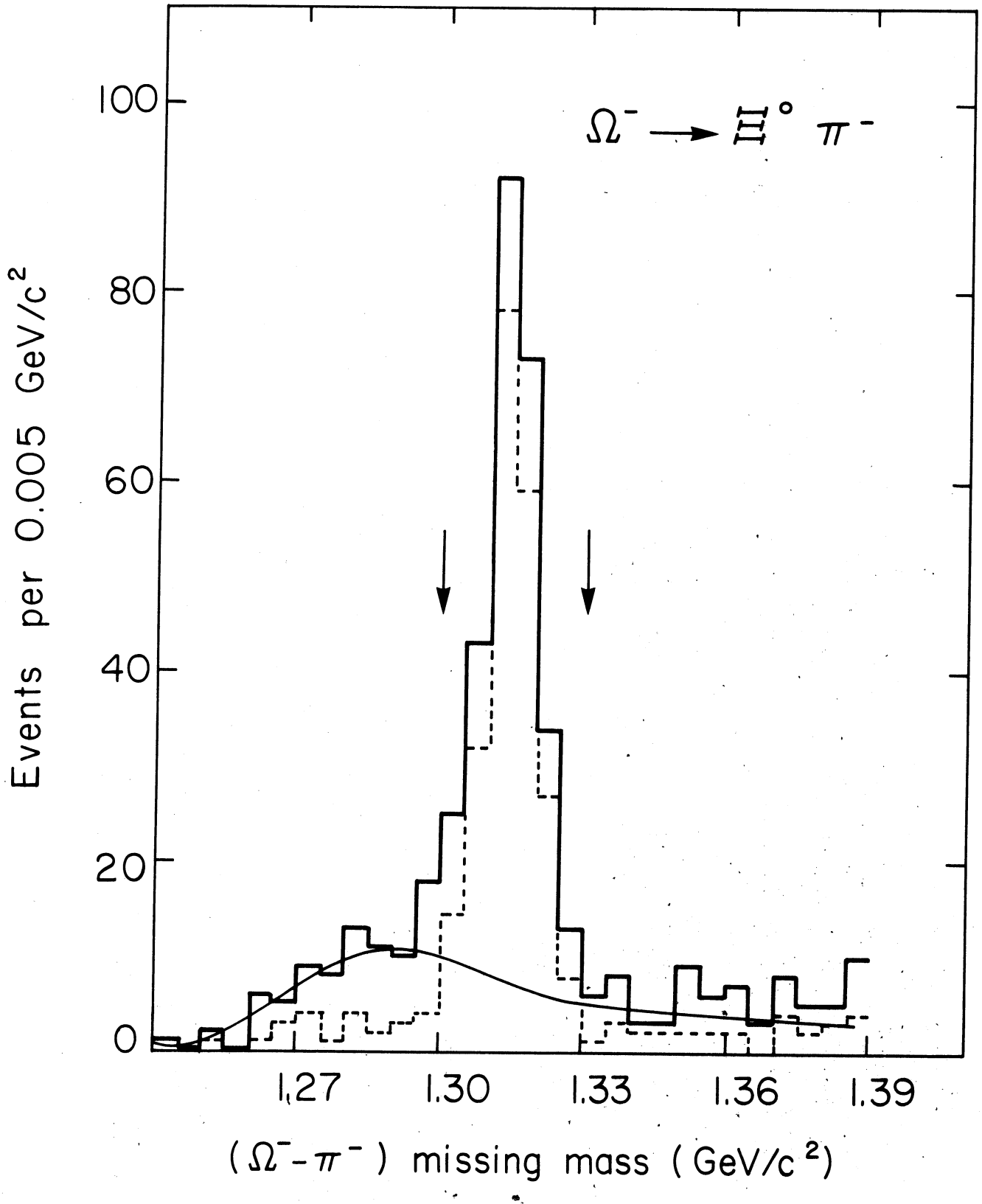
$\Omega^- \rightarrow \Xi^\circ \pi^-$
Events per 0.005 GeV/c^2
100
80
60
40
20
0
1.27
1.30
1.33
1.36
1.39
$(\Omega^- - \pi^-)$ missing mass (GeV/c^2)

Fig. 5

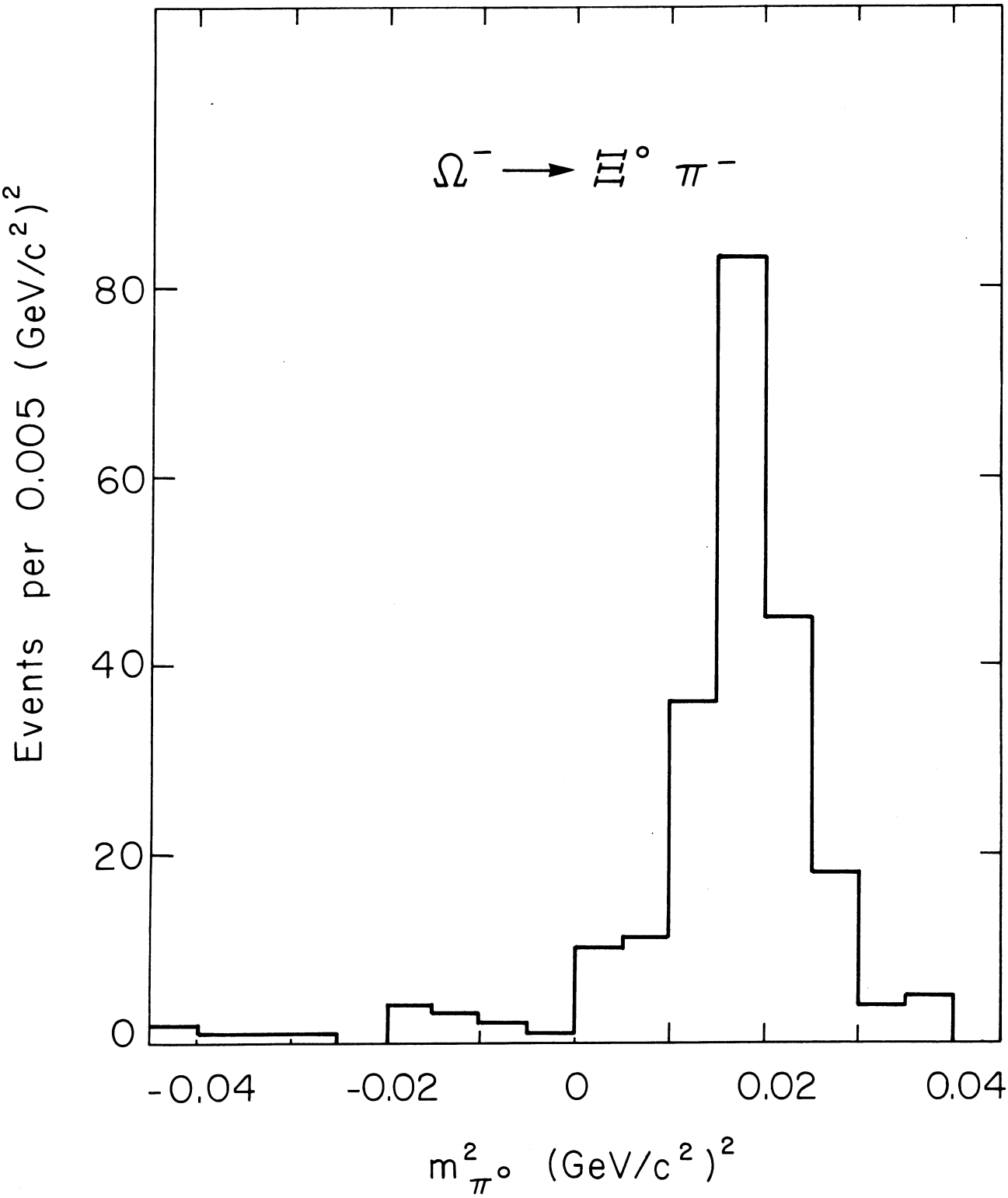
$\Omega^- \rightarrow \Xi^\circ \pi^-$
Events per 0.005 (GeV/c²)²
0
20
40
60
80
-0.04
-0.02
0
0.02
0.04
$m^2_{\pi^\circ}$ (GeV/c²)²

Fig. 6

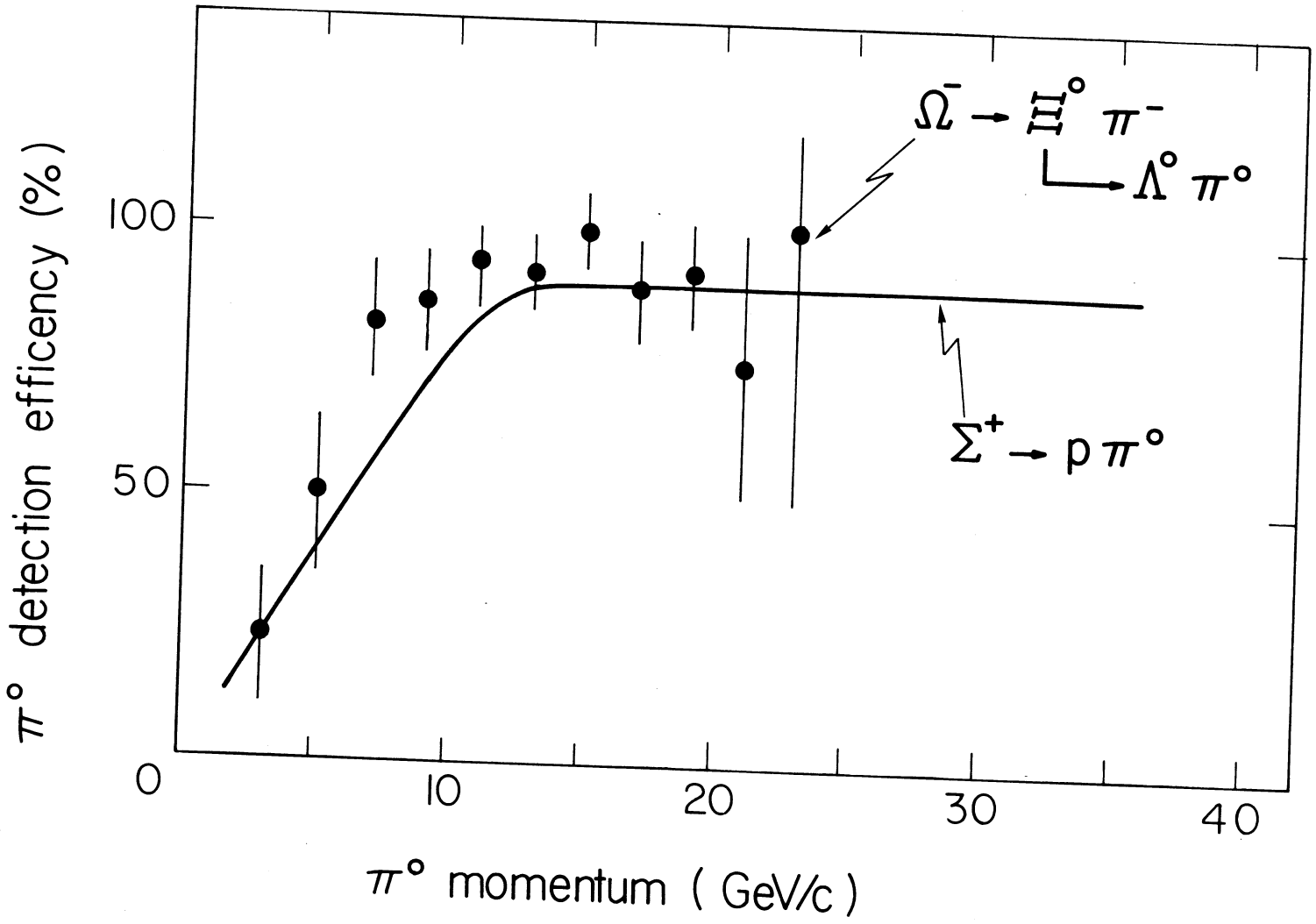
$\Omega^- \rightarrow \Xi^\circ \pi^-$
$\Lambda^\circ \pi^\circ$
$\Sigma^+ \rightarrow p \pi^\circ$
π° detection efficency (%)
100
50
0
10
20
30
40
π° momentum (GeV/c)

Fig. 7

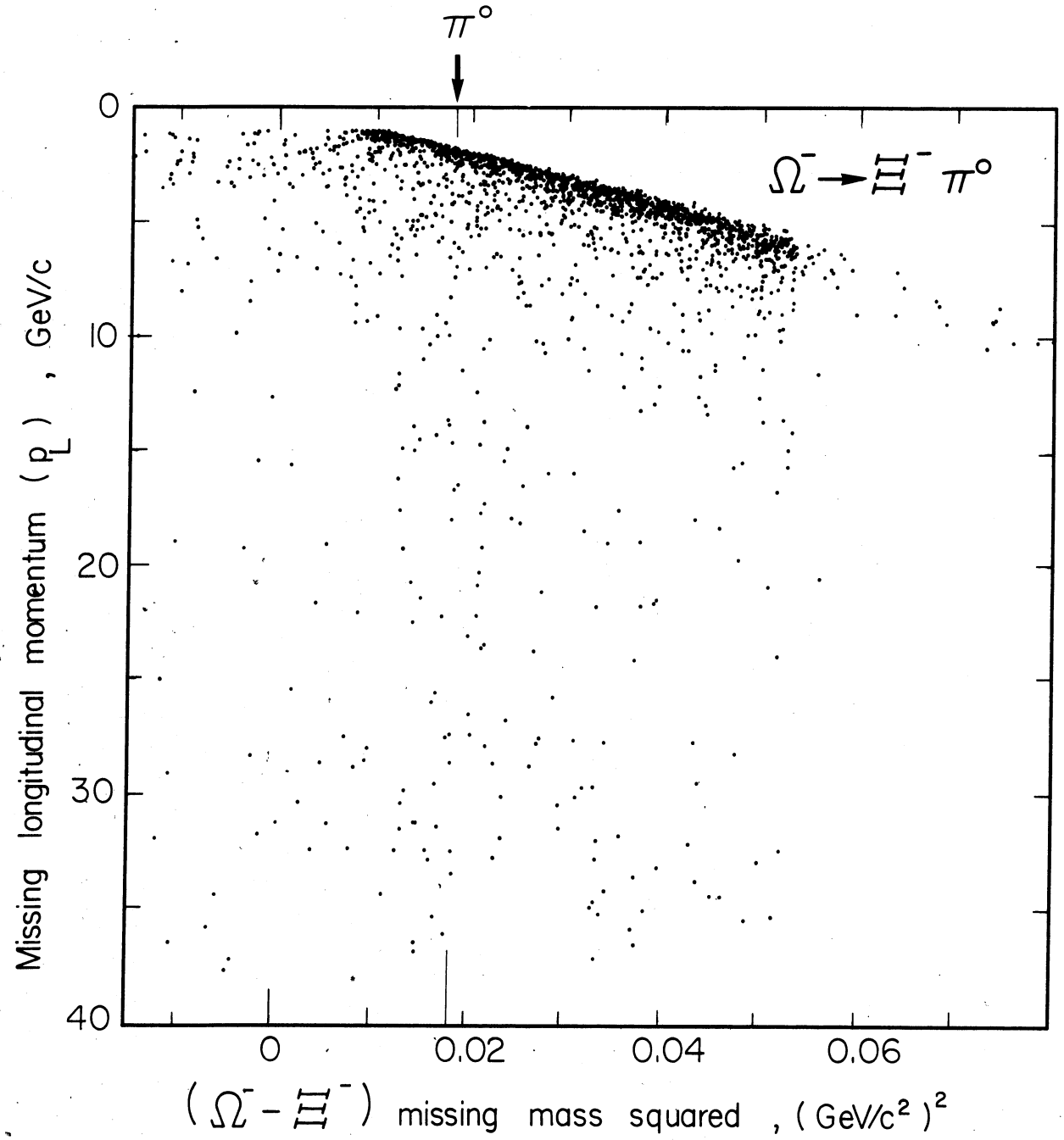
π°
Ω⁻ → Ξ⁻ π°
0
10
20
30
40
Missing longitudinal momentum (p_L) , GeV/c
0
0.02
0.04
0.06
(Ω⁻ − Ξ⁻) missing mass squared , (GeV/c²)²

Fig. 8

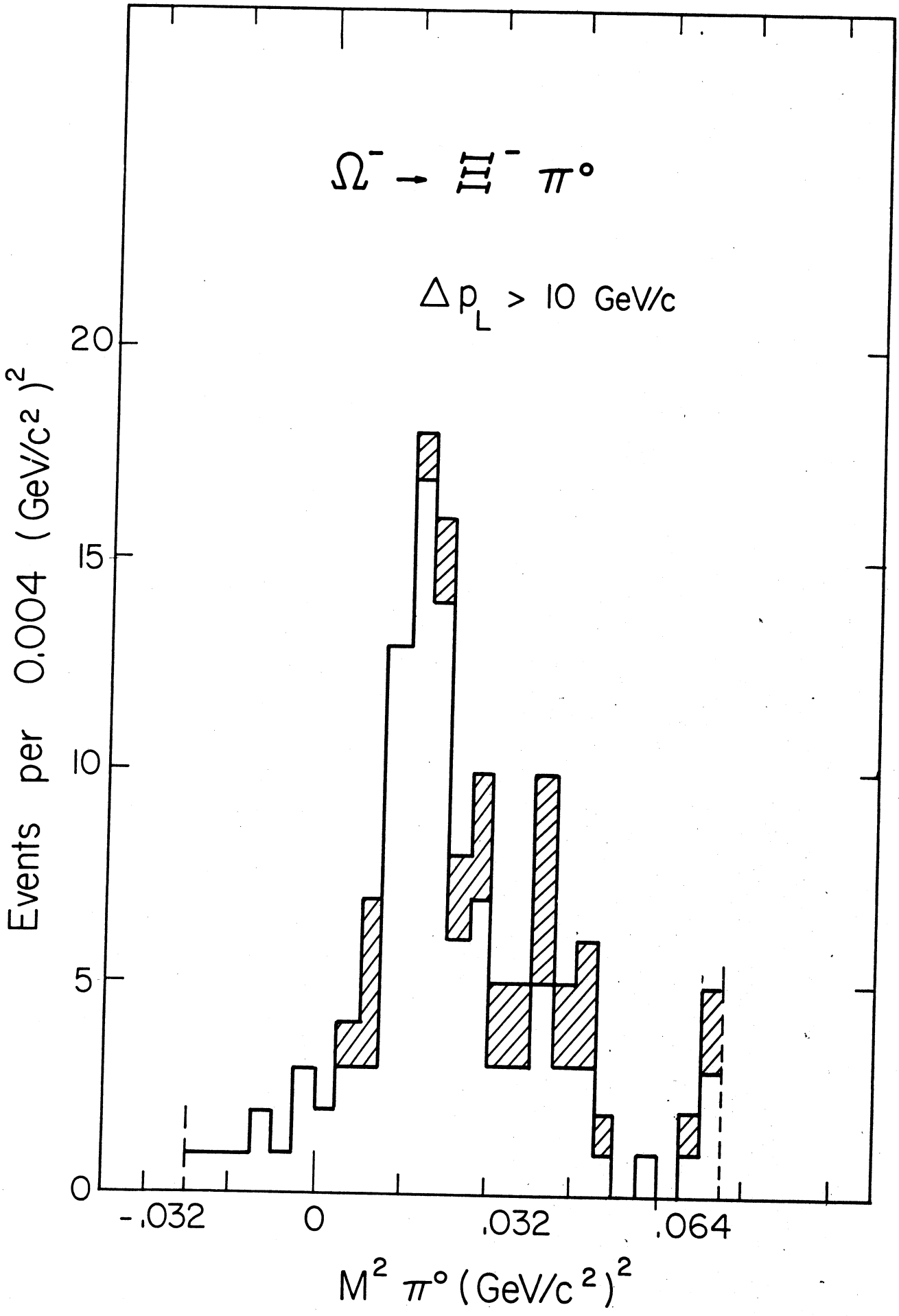
$\Omega^- \rightarrow \Xi^- \pi^\circ$
$\Delta p_L > 10$ GeV/c
Events per 0.004 (GeV/c²)²
20
15
10
5
0
-.032
0
.032
.064
$M^2 \pi^\circ$ (GeV/c²)²

Fig. 9

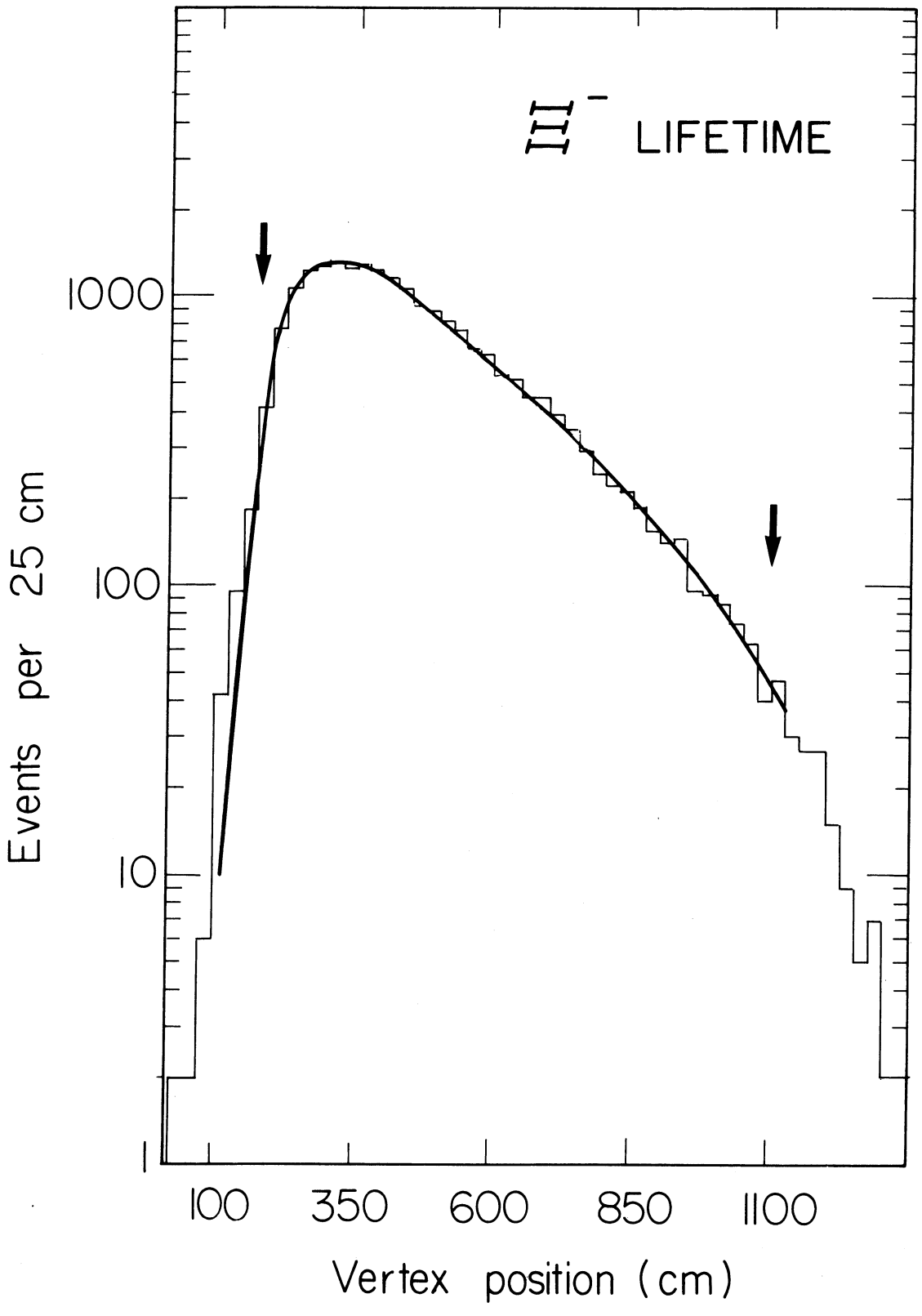
Ξ⁻ LIFETIME
1000
100
10
1
Events per 25 cm
100
350
600
850
1100
Vertex position (cm)

Fig.10

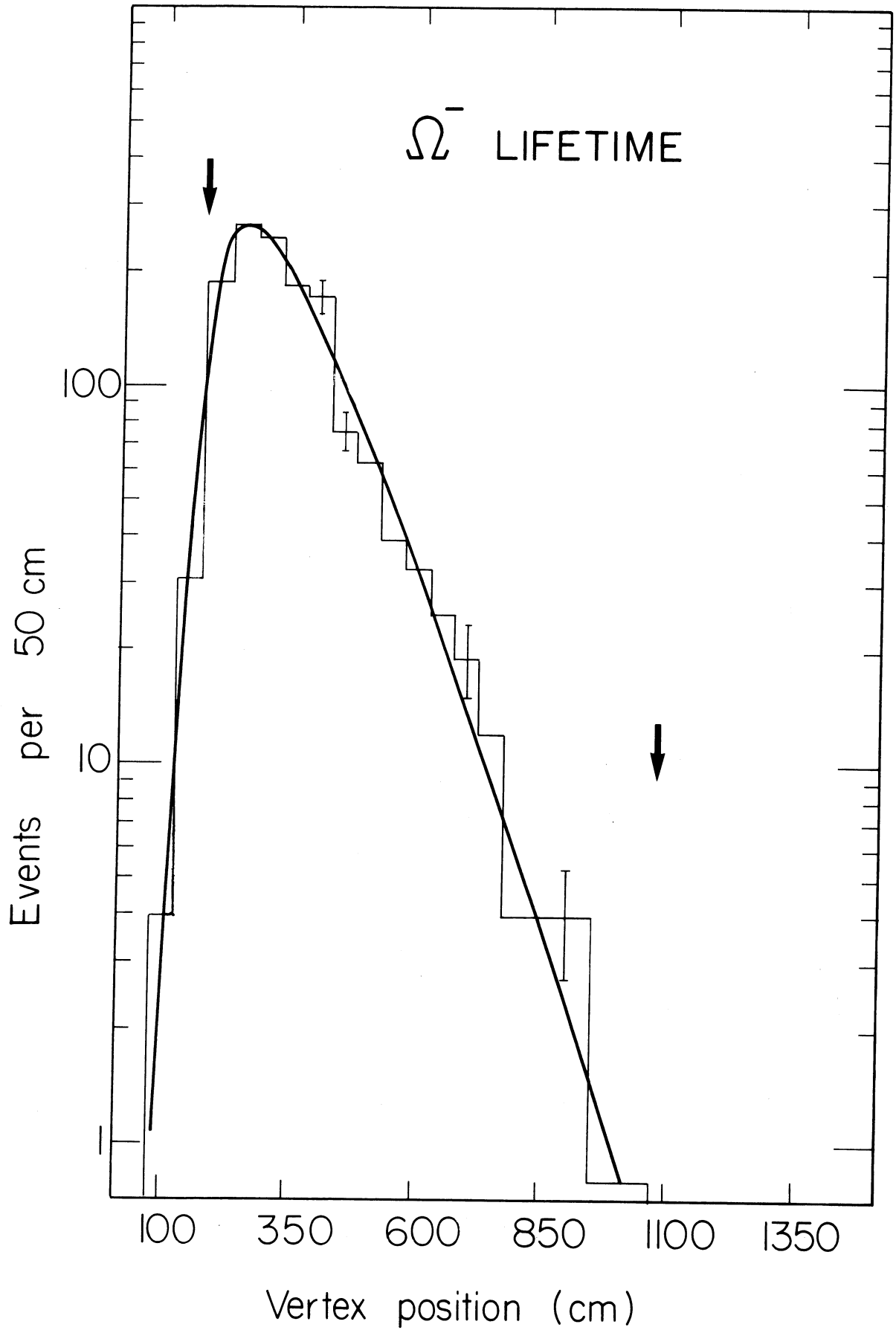
Ω^- LIFETIME
100
10
1
Events per 50 cm
100
350
600
850
1100
1350
Vertex position (cm)

Fig.11

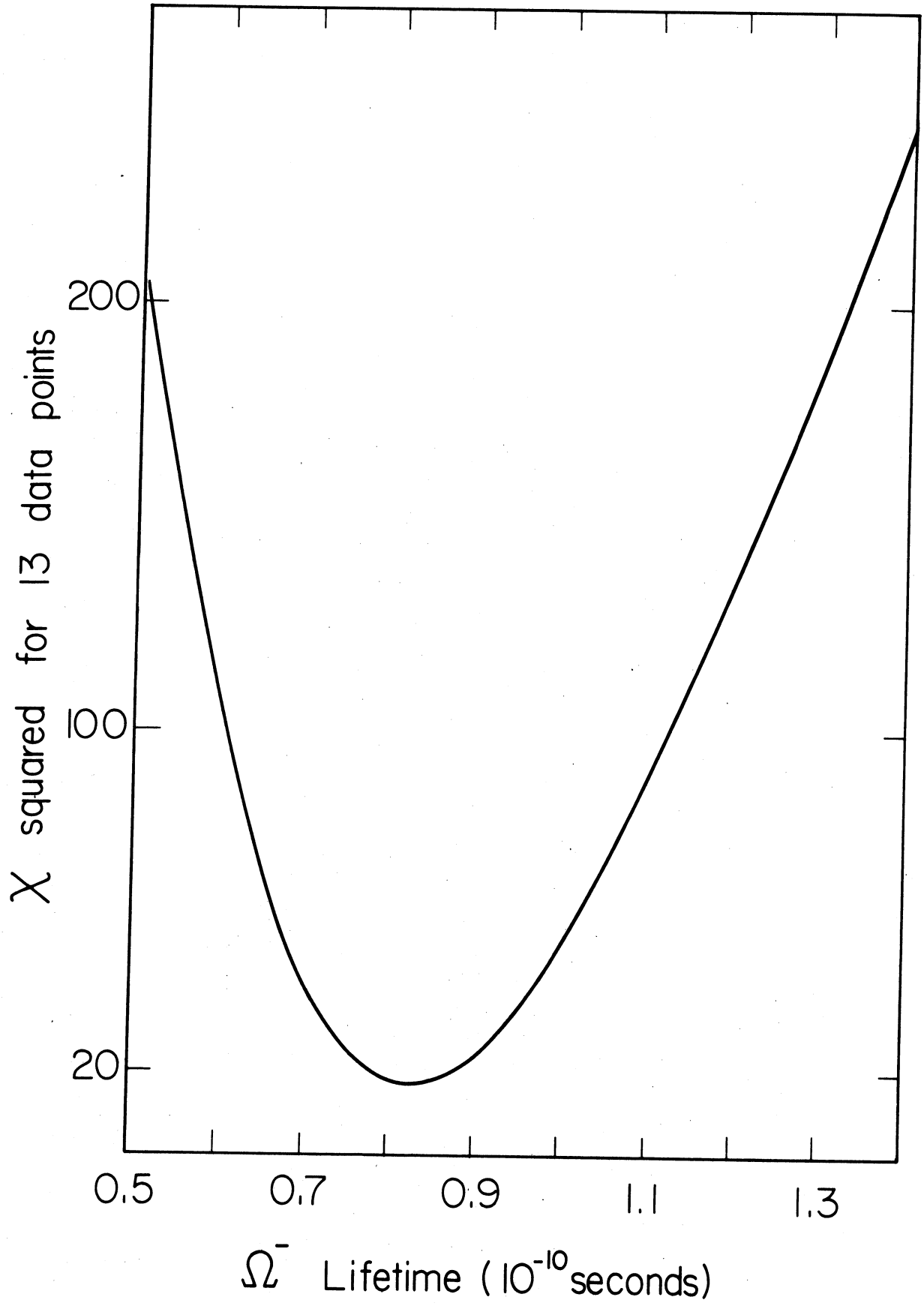
200
100
20
χ squared for 13 data points
0.5
0.7
0.9
1.1
1.3
Ω⁻ Lifetime (10⁻¹⁰ seconds)

Fig.12